Application of the parachor model to the prediction of miscibility in multi-component hydrocarbon systems

2004 J. Phys.: Condens. Matter 16 S2177

(http://iopscience.iop.org/0953-8984/16/22/017)

INSTITUTE OF PHYSICS PUBLISHING JOURNAL OF PHYSICS: CONDENSED MATTER

J. Phys.: Condens. Matter **16** (2004) S2177–S2186 PII: S0953-8984(04)75591-5

Application of the parachor model to the prediction of miscibility in multi-component hydrocarbon systems

Subhash C Ayirala and Dandina N Rao

The Craft and Hawkins Department of Petroleum Engineering, Louisiana State University, 3516 CEBA Building, Baton Rouge, LA 70803, USA

E-mail: dnrao@lsu.edu

Received 16 October 2003
Published 21 May 2004
Online at stacks.iop.org/JPhysCM/16/S2177
DOI: 10.1088/0953-8984/16/22/017

Abstract

While most thermodynamic properties refer to individual fluid phases, interfacial tension (IFT) is unique in the sense that it is a property of the interface between the fluid phases. The IFT, being a sensitive property strongly dependent on the composition of the interacting phases, is a good indicator of mass transfer effects between the phases. Furthermore, a condition of zero interfacial tension is essential to attain miscibility of the fluid phases in contact. Based on this concept, a new technique of vanishing interfacial tension (VIT) has been reported recently for experimental determination of fluid–fluid miscibility. Similar to the VIT technique in concept, a computational model based on parachor IFT calculations has been proposed in the present study for miscibility prediction. This model has been compared with VIT experiments and EOS calculations. For this purpose, Rainbow Keg River (RKR) reservoir fluids have been used, since the phase behaviour data necessary for miscibility calculations and the VIT experimental results were readily available.

The parachor computational model resulted in over-predictions of miscibility when compared to VIT experiments and EOS calculations. These over predictions appear to be due to the inability of the parachor model to account for counter-directional mass transfer effects that can occur in reality between the fluids. Thus, in addition to demonstrating the importance of counter-directional mass transfer effects on fluid–fluid miscibility, this study has identified the need to incorporate these mass transfer effects in the proposed parachor computational model to compute fluid–fluid miscibility.

(Some figures in this article are in colour only in the electronic version)

1. Introduction

1.1. Need for fluid–fluid miscibility

More than half of the crude oil found in petroleum reservoirs is left behind at the end of primary recovery and secondary water floods. This is due to rock–fluid interactions, including capillary forces, which prevent the oil from flowing within the pores of reservoir rock, trapping huge amounts of residual oil in reservoirs. These capillary forces can be reduced to a minimum if the interfacial tension between the injected fluid and the trapped crude oil is reduced to zero. Zero interfacial tension is nothing but miscibility between the injected fluid and reservoir crude oil [1–3]. Thus there is a need for miscibility development between the gas injected (natural gas or CO_2) and the crude oil to remobilize these huge amounts of trapped oil and improve the oil recovery.

1.2. Mass transfer mechanisms in miscibility development

Miscible displacement of crude oil in a reservoir can be carried out by the injection of gases such as hydrocarbon solvents, CO_2, flue gas and nitrogen. The compositional changes resulting from the mass transfer between reservoir oil and injected gas promote miscibility attainment. During displacements of oil by gas, miscibility develops mainly due to three types of mass transfer mechanism between the fluids in the reservoir, namely vaporizing gas drive, condensing gas drive and combined condensing/vaporizing gas drive.

In the vaporizing gas injection process, the injected gas is a relatively lean gas consisting of mostly methane and other low molecular weight hydrocarbons. As the injected fluid moves through the reservoir, it contacts the reservoir oil several times and becomes enriched in composition by vaporizing the intermediate components (C_2–C_4) in the crude oil. This process continues until the injected gas attains miscibility with reservoir oil.

In the condensing gas injection process, the injected gas contains significant amounts of intermediates (C_2–C_4). During the multiple contacts of the injected gas with crude oil in the reservoir, the intermediates condense from the gas phase into the oil phase. The continuation of this process modifies the reservoir oil composition to become miscible with additional injected gas, resulting in miscible displacement.

In the combined condensing/vaporizing process, the light intermediate compounds in the injected gas (C_2–C_4) condense into the reservoir oil, while the middle intermediate compounds (C_5–C_{10} to C_{30}) in the crude oil vaporize into the injected gas. This prevents miscibility between fluids near the injection point as the oil becomes heavier. As the injection of gas continues, there will be no further condensation of light intermediates from the injected gas into this saturated oil. However, the vaporization of middle intermediates continues from the oil enriching the injected gas further. As this condensation/vaporization process continues farther into the reservoir, the gas becomes enriched to greater and greater extents as it contacts more and more oil and eventually becomes miscible with the reservoir oil. This mechanism, involving simultaneous counter-directional mass transfer of components between the phases, is shown to be the one that most frequently occurs during the displacements of oil by gas [4].

2. Techniques to determine gas–oil miscibility

Minimum miscibility pressures (MMPs) and minimum miscibility enrichments (MMEs) are the important parameters for assessing miscibility conditions for displacements of oil by gas. The minimum miscibility pressure as the name implies is the lowest possible pressure

at which the injected gas (CO_2 or hydrocarbon) can achieve miscibility with reservoir oil at reservoir temperature. The minimum miscibility enrichment is the minimum possible enrichment of the injection gas with C_2–C_4 components at which miscibility can be attained with reservoir oil at reservoir temperature. Operating pressures below the MMP or injection gas enrichments below the MME result in immiscible displacements of oil by gas.

The primarily available experimental methods to evaluate miscibility under reservoir conditions are the slim-tube displacement, the rising bubble apparatus and the pressure composition diagrams. Apart from these experimental techniques, several computational models are also available to determine fluid–fluid miscibility. The most important among these models are the equation of state (EOS) calculations and analytical models based on tie-line length calculations.

Recently a new experimental technique of vanishing interfacial tension (VIT) has been reported for fluid–fluid miscibility evaluation [5, 6]. This technique relies on the concept that the interfacial tension between the fluids must reduce to zero as the fluid phases approach the point of miscibility. In this method, the interfacial tension is measured between the injected gas and crude oil at reservoir temperature at varying pressures or enrichment levels of the gas phase. The MMP or MME is then determined by extrapolating the plot between interfacial tension and pressure or enrichment to zero interfacial tension. None of the previously mentioned experimental techniques provide such direct and quantitative information on interfacial tension. In addition to being quantitative in nature, this new VIT technique is quite rapid as well as cost effective.

With the equation of state (EOS) model, the predictions of phase behaviour have become more reliable due to advances in computer-implementation of iterative vapour–liquid equilibrium flash calculations. However, this approach requires large amounts of compositional data of the reservoir fluids for computations, which have to be obtained from laboratory PVT measurements.

In addition to using the existing computational EOS models, another model based on parachor IFT calculations has been investigated in this study for miscibility prediction. Just as the VIT experimental technique, this model is also based on the concept of zero interfacial tension at miscibility. In this model, the interfacial tension between the fluids is calculated using Weinaug and Katz's [7] parachor method at reservoir temperature as a function of pressure or gas enrichment. Then the extrapolation of the plot between interfacial tension and pressure or enrichment to zero interfacial tension yields the conditions of miscibility.

The objectives of this investigation are to utilize the parachor model to calculate interfacial tension in complex vapour–liquid systems involving multi-components in both phases and to evaluate the performance of the proposed parachor model by comparing the miscibility conditions of pressure and enrichment determined from the model with VIT experiments and equation of state (EOS) calculations. For this purpose, Rainbow Keg River (RKR) reservoir fluids were used, since all the phase behaviour data needed for miscibility calculations and the VIT experimental results were readily available [5, 6]. The calculations were carried out using the commercial simulator Winprop [8].

3. Equation of state (EOS) calculations

Our previous study on the effects of tuning an equation of state (EOS) on miscibility calculations [9] indicates that EOS tuning based on saturation pressures is not suitable for miscibility calculations of this reservoir fluid. Hence, the untuned Peng–Robinson EOS has been chosen in the present study to perform all the calculations. The reservoir fluid composition, reservoir temperature, the composition of lean and rich gases used for

Table 1. Composition of Rainbow Keg River reservoir fluids used. (Note: reservoir temperature: 188 °F; saturation pressure (bubble point): 2486.7 psia; reservoir pressure: 2538.6 psia.)

Component	mol% in crude oil[a]	mol% in lean gas (primary)	mol% in rich gas (makeup)	Solvent no 1	Solvent no 2
Hydrogen sulfide	1.37	0.00	0.00	0.00	0.00
Carbon dioxide	0.82	1.24	0.80	1.02	1.01
Nitrogen	0.57	1.76	0.40	1.08	1.05
Methane	35.13	81.01	14.73	47.92	46.45
Ethane	10.15	11.14	21.34	16.23	16.46
Propane	6.95	3.95	41.83	22.86	23.70
iso-butane	1.10	0.50	7.35	3.92	4.07
n-butane	3.16	0.34	11.67	6.00	6.25
iso-pentane	2.29	0.00	0.00	0.00	0.00
n-pentane	1.74	0.07	1.89	0.98	1.02
Hexanes	3.68	0.00	0.00	0.00	0.00
Heptanes plus	33.04	0.00	0.00	0.00	0.00
Total	100	100	100	100	100
$C_{2+} + CO_2$	62.93	17.24	84.88	51.00	52.50
Makeup (%)				49.92	52.14

[a] Properties of C_{7+} in crude oil: specific gravity: 0.8397; molecular weight: 205.

making up the solvent and the solvent compositions described in table 1 form the basis for this study.

3.1. MMP calculations

The following steps are used to calculate MMPs at the reservoir temperature.

(1) An initial pressure below the MMP is chosen to start the computation.
(2) The reservoir temperature, crude oil composition, primary and makeup gas compositions, makeup gas fraction, pressure increment, solvent to oil ratio increment, equilibrium gas/original oil mixing ratio and equilibrium liquid/original solvent mixing ratio are then provided as inputs to the program.
(3) The composition of solvent obtained by mixing of primary and makeup gases is then calculated using the specified ratio.
(4) Solvent is added to the crude oil at specified solvent to oil molar ratio increments and flash calculations are performed until the two-phase region is detected. The absence of the two-phase region implies first contact miscibility and the program stops.
(5) For the presence of the two-phase region, the program checks the relative positions of solvent and crude oil compositions with respect to limiting tie line. If the solvent composition is to the left, while that of crude oil is to the right of the limiting tie line, then the process is a vaporizing gas drive. Otherwise, the process is a condensing gas drive [10].
(6) For a vaporizing gas drive, using the first point in the two-phase region detected in step 4, the flashed vapour is mixed with the original oil at the specified ratio of equilibrium gas to original oil and the flash calculation is performed.
(7) For a condensing gas drive, using the first point in the two-phase region detected in step 4, the flashed liquid is mixed with the original solvent at the specified ratio of equilibrium liquid to original solvent and the flash calculation is performed.

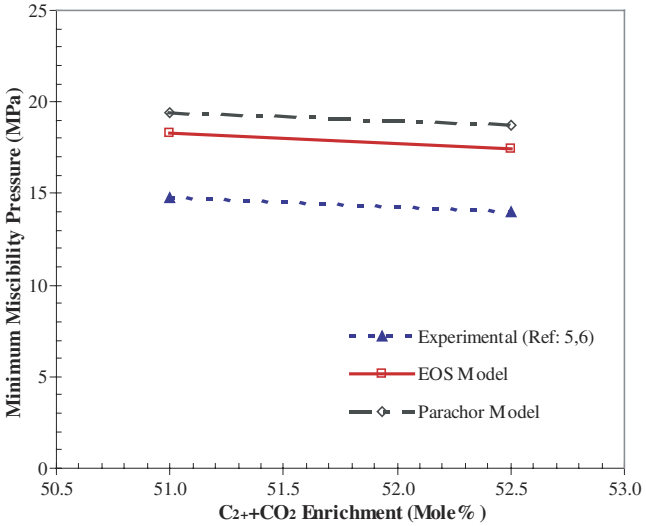

Figure 1. Comparison of VIT MMPs with EOS calculations and the parachor model.

Table 2. Comparison of VIT MMPs with EOS calculations and the parachor model.

MMP determination method	Solvent no 1 ($C_{2+} = 51.0\%$) MMP (MPa)	Solvent no 2 ($C_{2+} = 52.5\%$) MMP (MPa)
Experimental (VIT) [5, 6]	14.8	14.0
PR–EOS calculation	18.3	17.4
Parachor model (Weinaug and Katz)	19.4	18.7

(8) The procedure is repeated until the liquid composition is the same as the vapour composition and the MMP is the pressure at which this occurs and the program stops.
(9) Otherwise, the pressure is increased at a specified pressure increment and steps 4 to 8 are repeated.

The comparison between the MMPs from VIT experiments and EOS calculations for RKR fluid at C_{2+} enrichments of 51.0% and 52.5% in the injected gas phase (solvent) is given in table 2 and shown in figure 1. From these results, it can be seen that the EOS MMP predictions are higher than the experimental MMPs (by about 3.5 MPa). This is in good agreement with other reports [11, 12] that EOS calculations yield more conservative results than laboratory measurements.

4. Parachor computational model

4.1. Background

Macleod–Sudgen [13, 14] related surface tension of a pure compound to the density difference between the phases as:

$$\sigma^{1/4} = P(\rho_{\mathrm{M}}^{\mathrm{L}} - \rho_{\mathrm{M}}^{\mathrm{V}}) \tag{1}$$

where σ is the surface tension in dyn cm^{-1}, $\rho_{\mathrm{M}}^{\mathrm{L}}$ and $\rho_{\mathrm{M}}^{\mathrm{V}}$ are the molar density of the liquid and vapour phases, respectively, in g mol cm^{-3} and the proportionality constant, P is known

Table 3. Comparison of measured IFTs with the parachor model predictions.

Pressure = 14.8 MPa			Pressure = 14.0 MPa		
	IFT (dyn cm^{-1})			IFT (dyn cm^{-1})	
Enrichment (C_{2+}%)	Experimental [5, 6]	Parachor	Enrichment (C_{2+}%)	Experimental [5, 6]	Parachor
17.79	4.26	2.91	32.68	2.86	1.88
21.64	3.89	2.59	37.55	1.89	1.46
25.85	3.27	2.21	41.45	1.51	1.14
30.57	2.69	1.81	42.61	1.39	1.04
33.86	2.13	1.54	47.48	0.70	0.68
37.70	1.52	1.24			
43.07	0.97	0.85			
48.39	0.53	0.50			
49.28	0.27	0.48			

as the parachor. The parachor values of various pure compounds have been determined from measured surface tension data using equation (1). The parachor values of different pure compounds are reported in the literature by several investigators [15–18].

The equation proposed by Macleod–Sudgen [13, 14] was later extended to hydrocarbon mixtures using the simple molar averaging technique of Weinaug and Katz [7] for the mixture parachor,

$$\sigma^{1/4} = \rho_{\mathrm{M}}^{\mathrm{L}} \sum x_i P_i - \rho_{\mathrm{M}}^{\mathrm{V}} \sum y_i P_i \tag{2}$$

where x_i and y_i are the mole fractions of component i in the liquid and vapour phases, respectively, and P_i is the parachor of the component i. Parachor values of pure compounds are used in equation (2) to calculate the interfacial tension of the mixtures, considering the parachor value of a component in a mixture is the same as that when pure [19]. This method is most widely used in the petroleum industry to estimate the interfacial tension between fluids.

4.2. Gas–oil IFT calculations

In order to apply the parachor model to the current reservoir case study, a mixture consisting of 10 mol% of crude oil and 90 mol% of solvent is used as the feed composition in the computational model to match the composition used in VIT experiments. Flash calculations are performed with the mixed feed at the specified pressure and reservoir temperature at varying C_{2+} enrichments in solvent. The resultant molar liquid, vapour densities, equilibrium liquid and vapour compositions of different components along with their parachors reported in the literature, are then used in IFT computations.

The summary of experimental IFTs and the calculated IFTs using the parachor computational model for RKR fluids at different C_{2+} enrichments in solvent is given in table 3 for pressures of 14.8 and 14.0 MPa. Similar trends are observed at both the pressures. The parachor computational model under-predicts the interfacial tension in high IFT regions. However, the difference between the experimental and the calculated IFTs gradually decreases and consequently the parachor model predictions match with experimental measurements in the low IFT regions. This is in good agreement with Cornelisse *et al* [20] where similar observations are made. The calculated IFTs are then plotted against C_{2+} enrichment to determine MMEs in figures 2 and 3, for pressures of 14.8 and 14.0 MPa, respectively. As can be seen in these figures, conservative estimates of MMEs are obtained with the parachor model when compared to experimental MMEs (by about 3.2–3.4%) at both pressures.

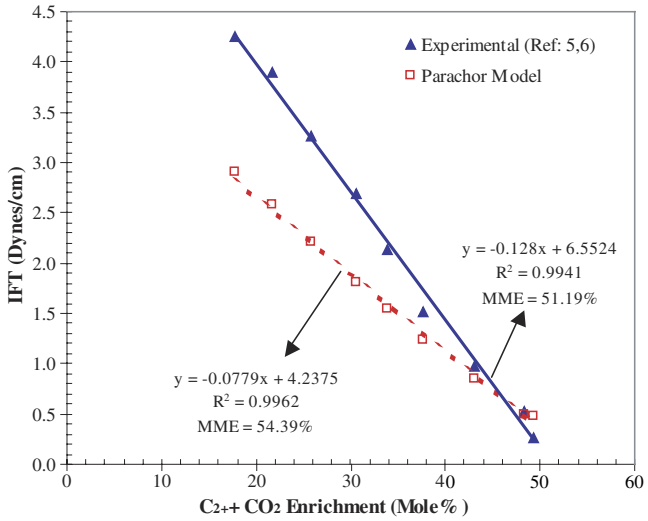

Figure 2. Comparison of experimental IFTs with the parachor model for RKR fluids at a pressure of 14.8 MPa.

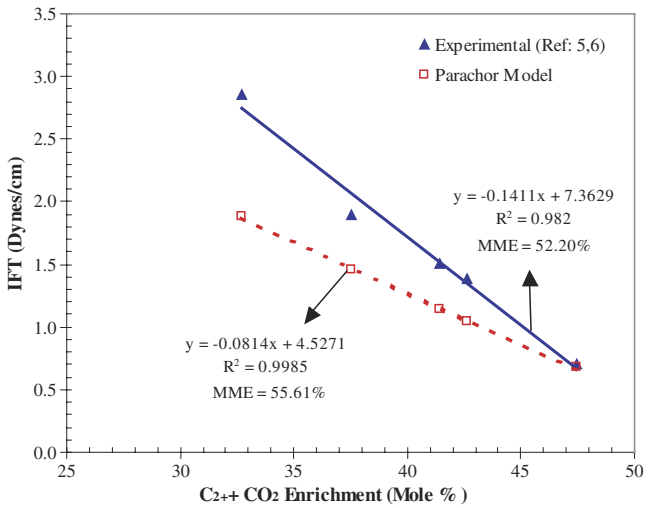

Figure 3. Comparison of experimental IFTs with the parachor model for RKR fluids at a pressure of 14.0 MPa.

4.3. MMP calculations

The sequence of steps followed in the MMP calculation procedure using the parachor computational model are:

(1) Oil composition, solvent composition, reservoir temperature, mole fraction of oil in the feed, pressure and the pressure increment are provided as inputs to the model.
(2) Flash calculations are performed with mixed feed at reservoir temperature and specified pressure.

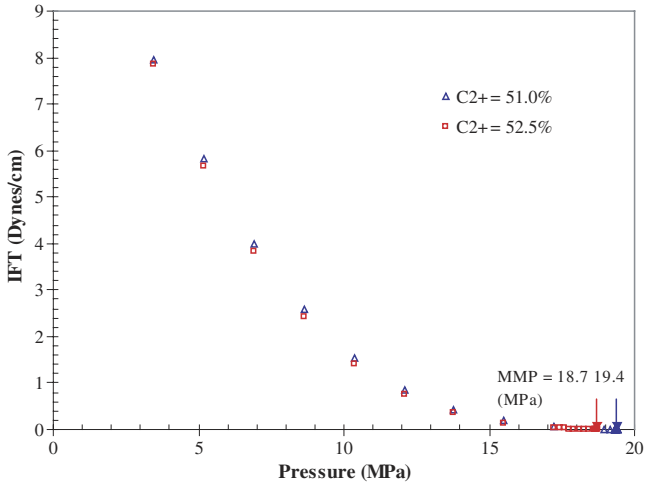

Figure 4. MMP determination using the parachor computational model for RKR fluids.

(3) The resulting molar liquid, vapour densities, equilibrium liquid and vapour compositions of different components along with their parachors are used to calculate the IFTs.
(4) The pressure is incremented at the specified pressure increment and steps 2 to 3 are repeated.
(5) In the low interfacial tension region, pressure is incremented in smaller steps to clearly identify the point of vanishing IFT pressure. Then this vanishing IFT pressure becomes the MMP for the system.

The comparison between VIT experimental MMPs and the calculated MMPs from the parachor computational model for RKR fluids at C_{2+} enrichments of 51.0% and 52.5% in solvent is given in table 2 and shown in figure 1. The calculated IFTs using the parachor model at these C_{2+} enrichments are plotted against pressure to determine MMPs in figure 4. From these results, it is quite evident that the parachor model resulted in MMP over-predictions, when compared to VIT experiments (by about 4.5 MPa). Moreover, these over-predictions are greater than those obtained in EOS calculations.

5. Mass transfer effects on miscibility predictions

Since IFT, a good indicator of mass transfer effects, was used to interpret miscibility in this study, the reasons for the miscibility over-predictions by the computational models appear to be the following.

In VIT experiments, equilibrated fluids are used in IFT measurements. Hence various types of mass transfer mechanisms are allowed to take place between the fluids (condensing gas drive, vaporizing gas drive and combined condensing/vaporizing gas drive). Thus VIT measurements include all the mass transfer effects and hence predict true MMPs. In EOS calculations, mass transfer effects are taken into account only through either a condensing gas drive or a vaporizing gas drive, which is quite evident in the MMP calculation procedure of the EOS model. This limited mass transfer resulted in MMP over-predictions (about 3.5 MPa) by the EOS model. In the parachor computational model, the parachor values are based on surface tension measurements of pure compounds. Hence these values are incorporated into the computational model considering each component of the mixture as if all the others were

absent. Because of this assumption, any type of mass transfer effect is not considered at all in the calculation procedure. This appears to be responsible for even larger over-predictions of the MMP (about 4.5 MPa) by the parachor model.

Further, it can be seen that the difference in the over-predictions of miscibility is not significant (only about 1 MPa) between the EOS and parachor models. This means incorporation of either a condensing or vaporizing mass transfer mechanism in the EOS model has not resulted in any significant improvement in accuracy of miscibility prediction. This observation intuitively suggests that the combined vaporizing/condensing mechanism involving simultaneous counter-directional mass transfer of components between the fluid phases is the main mechanism that controls fluid–fluid miscibility. This is in good agreement with the experimental observations of Zick [4]. Thus the ability of any miscibility computational procedure to account for the counter-directional mass transfer effects between the fluids governs the extent of agreement with miscibility pressures and enrichments determined from VIT experiments. This clearly demonstrates the importance of mass transfer effects in fluid–fluid miscibility computations and hence identifies the need to develop methods to incorporate these mass transfer effects in the models used to compute miscibility.

6. Conclusions

(1) The interfacial tensions computed using the parachor model are found to differ from the experimental measurements by more than 1.0 dyn cm^{-1} when the IFT is above 3 dyn cm^{-1} and as low as 0.1 dyn cm^{-1} when the IFT is below 3 dyn cm^{-1}.

(2) The parachor computational model over-predicts minimum miscibility pressures when compared to VIT experiments (by about 4.5 MPa) and EOS calculations (by about 1.0 MPa).

(3) The combined vaporizing/condensing mechanism involving simultaneous counter-directional mass transfer of components between the fluid phases appears to be the main mass transfer mechanism that governs the attainment of fluid–fluid miscibility.

(4) The disagreement with IFT measurements and over-predictions of miscibility conditions obtained using the proposed parachor model appears to be due to the inability of the model to account for counter-directional mass transfer effects that can occur in reality between the fluids.

(5) This study exemplifies the importance of counter-directional mass transfer effects in interfacial phenomena and hence gives rise to the need to develop methods to incorporate these mass transfer effects in the proposed parachor model for interfacial tension and miscibility calculations.

Acknowledgments

This paper was prepared with the support of the US Department of Energy under Award No DE-FC26-02NT-15323. Any opinions, findings, conclusions or recommendations expressed herein are those of authors and do not necessarily reflect the views of the DOE. The financial support of this project by the US Department of Energy is gratefully acknowledged. The authors thank Dr Jerry Casteel of NPTO/DOE for his support and encouragement. Sincere thanks are due to Husky Oil Operations for providing the necessary PVT data of the crude oils used. We thank David Fong and Frank Mcintyre of Husky Oil for helpful discussions.

References

[1] Holm L W 1987 Miscible displacement *Petroleum Engineering Hand Book* ed H B Bradley (Richardson, TX: Society of Petroleum Engineers) pp 1–45

[2] Lake L W 1989 *Enhanced Oil Recovery* (Englewood Cliffs, NJ: Prentice-Hall) p 234

[3] Benham A L, Dowden W E and Kunzman W J 1965 *Miscible Fluid Displacement—Prediction of Miscibility* (*Petroleum Transactions Reprint Series No. 8*) (Richardson, TX: Society of Petroleum Engineers of AIME) p 123

[4] Zick A A 1986 A combined condensing/vaporizing mechanism in the displacement of oil by enriched gases *SPE 61st Annual Technical Conf. and Exhibition (New Orleans, LA, Oct. 1986)* Paper SPE 15493

[5] Rao D N 1997 A new technique of vanishing interfacial tension for miscibility determination *Fluid Phase Equilib.* **139** 311–24

[6] Rao D N, Mcintyre F J and Fong D K 1999 Application of a new technique to optimize injection gas composition for the Rainbow Keg River F Pool miscible flood *J. Canadian Petroleum Technol.* **38** 1–10

[7] Weinaug C F and Katz D L 1943 Surface tensions of methane–propane mixtures *Indust. Eng. Chem.* **35** 239–46

[8] *Winprop Phase Property Program, Version 2001 User's Guide,* Computer Modeling Group, Calgary, Canada

[9] Ayirala S C, Rao D N and Casteel J F 2003 Comparison of minimum miscibility pressures determined from gas–oil interfacial tension measurements with equation of state calculations *SPE Annual Technical Conf. and Exhibition (Denver, CO, Oct. 2003)* Paper SPE 84187

[10] Green D W and Willhite G P 1998 *Enhanced Oil Recovery* vol 6 (Richardson, TX: Society of Petroleum Engineers of AIME) pp 186–238

[11] Lee J I and Reitzel G A 1982 High pressure, dry gas miscible flood—Brazeau River Nisku Oil Pools *J. Petroleum Technol.* **34** (November) 2503–9

[12] Firoozabadi A and Aziz K 1986 Analysis and correlation of nitrogen and lean gas miscibility pressure *SPERE* (August) 100–10

[13] Macleod D B 1923 On a relation between surface tension and density *Trans. Faraday Soc.* **19** 38–42

[14] Sudgen S 1924 The variation of surface tension with temperature and some related functions *J. Chem. Soc.* **125** 32–41

[15] Quale O R 1953 The parachors of organic compounds *Chem. Rev.* **53** 439–586

[16] Fanchi J R 1990 Calculation of parachors for compositional simulation: an update *SPE Reservoir Eng.* **5** 433–6

[17] Ali J K 1994 Predictions of parachors and petroleum cuts and pseudo components *Fluid Phase Equilib.* **95** 383–98

[18] Schechter D S and Guo B 1998 Parachors based on modern physics and their uses in IFT prediction of reservoir fluids *SPE Reservoir Eval. Eng.* **1** 207–17

[19] Danesh A 1998 *PVT and Phase Behavior of Petroleum Reservoir Fluids* (Amsterdam: Elsevier Science B.V.) pp 281–99

[20] Cornelisse P M W, Peters C J and de Swaan Arons J 1993 Application of the Peng–Robinson equation of state to calculate interfacial tensions and profiles at vapor–liquid interfaces *Fluid Phase Equilib.* **82** 119–29